Development of a Remote Monitoring System for Respiratory Analysis

Atena Roshan Fekr(✉), Majid Janidarmian, Katarzyna Radecka, and Zeljko Zilic

Department of Electrical and Computer Engineering, McGill University, Montreal, QC, Canada
{atena.roshanfekr,majid.janidarmian}@mail.mcgill.ca, {katarzyna.radecka,zeljko.zilic}@mcgill.ca

Abstract. In order to prevent the lack of appropriate respiratory ventilation which causes brain damage and critical problems, it is required to continuously monitor the breathing signal of a patient. There are different conventional methods for capturing respiration signal, such as polysomnography and spirometer. In spite of their accuracy, these methods are expensive and could not be integrated in a body sensor network. In this work, we present a real-time cloud-based respiration monitoring platform which allows the patient to continue treatment and diagnosis from different places such as home. These remote services are designed for patients who suffer from breathing problems or sleep disorders. Our system includes calibrated accelerometer sensor, Bluetooth Low Energy (BLE) and cloud database. Based on the high correlation between spirometer and accelerometer signals, the Detrended Fluctuation Analysis (DFA) has been applied on respiration signals. The obtained results show that DFA can be used as an efficient feature while classifying the healthy people from patients suffering from breath abnormalities.

Keywords: Breath analysis · Detrended fluctuation analysis · Accelerometer sensor

1 Introduction

Recently, there are different studies and reports which show the importance of monitoring and analyzing the respiration signals in many fields such as medicine and physiology [1–4]. Today about 7 % of the population of developed countries suffer from Chronic Obstructive Pulmonary Disease (COPD), and it is a growing problem in developing countries. For example, an estimated of 3.7 million people live with COPD in UK, predicted to increase by one-third by 2030, costing the NHS £1.2 billion/yr [3]. Moreover, professionals in breathing and sleep centers are demanded to assist people with shortness of breath, cardiovascular problems, such as hypertension, atherosclerosis, stroke, heart failure, cardiac arrhythmias, and sudden infant death syndrome (SISD). Therefore, a real-time monitoring of the respiration rhythm plays an important role in both diagnosis and treatment of different disorders. Remote monitoring also helps in prevention and early diagnosis of adult diseases, such as obesity, diabetic ketoacidosis

R. Giaffreda et al. (Eds.): IoT360 2014, Part I, LNICST 150, pp. 193–202, 2015.
DOI: 10.1007/978-3-319-19656-5_28

(DKA), brain disorders as well as abnormal breathing of newborns at home. There are different conventional methods for respiration waveform measurement, such as spirometry, nasal thermocouples, impedance plethysmography, inductance pneumography strain gauge measurements of thoracic circumference, whole-body plethysmography [4], pneumatic respiration transducers, the fiber-optic sensor method [4, 5], the Doppler radar [5, 6], and electrocardiogram (ECG)-based derived respiration measurements [7–9]. However, in spite of their accuracies, these methods are expensive and inflexible which may bring discomfort to the patients and physicians. One recent area of interest is applying motion sensors to detect the small movements of the chest wall that occur during expansion and contraction of the lungs. In preliminary trials on hospital patients, it has been shown that [10] with proper signal processing, this method can produce results that closely match with measurements of nasal cannula pressure [10]. A validation of respiratory signal derived from suprasternal, notch acceleration has been investigated by [11] for different body positions. Their data storage and processing is performed on a computer with their custom build LabVIEW Virtual Instrument. The main objective of this study is to provide a new cloud-based tool for monitoring and analyzing the respiration patterns with accelerometer sensor. The previous approaches are primarily based on the use of offline data loggers and on-board signal processing. However, in our system we use cloud database which can offer significant advantages over traditional methods, including increased on-line accessibility, scalability, automatic failover and fast automated recovery from failures. The accelerometer data is transmitted via Bluetooth Low Energy (BLE) to PC/iPhone and then it is sent to the cloud to be processed and saved, immediately. Therefore, the physicians can track the patients wherever they are with devices such as an iPhone, iPad or the web regardless of their proximity to the patients. Moreover the fluctuation analysis of the signals for each patient is investigated as an effective feature to distinguish breath problems.

In Sect. 2, the signal processing procedures applied on accelerometer signal are explained. In Sect. 3, the Detrended Fluctuation Analysis (DFA) has been applied on respiration signals derived from the accelerometer to help distinguishing between normal and abnormal respiration patterns. Experimental results are presented and discussed in Sect. 4. Finally Sect. 5 concludes the paper.

2 Data Preprocessing

We mounted the sensor on the chest where is more comfortable compared to suprasternal notch position used in [11]. In order to make sure that the sensors' readings are accurate enough to be processed, we calibrate our accelerometer sensor using linear least square method proposed by [12]. Due to inherent deficiency or aging problems in cyber-biological systems, sensors calibration is suggested. Calibration, which is defined as the process of mapping raw sensor readings into corrected values, can be used to compensate the systematic offset and gain [13]. Generally, calibration of sensors requires experience and special accurate tools; however, a straightforward method to calibrate an accelerometer is performed at 6 stationary positions. We need to collect a few seconds of accelerometer raw data at each position. Then the least square method is applied to obtain the 12 accelerometer calibration parameters. The calibration

procedure is simple, and needs to be executed once. The calibration procedure can be briefly explained as:

$$\left[a_{x'} a_{y'} a_{z'}\right] = \left[a_x\, a_y\, a_z\, 1\right].\begin{bmatrix} acc_{11}\, acc_{21}\, acc_{31} \\ acc_{12}\, acc_{22}\, acc_{32} \\ acc_{13}\, acc_{23}\, acc_{33} \\ acc_{10}\, acc_{20}\, acc_{30} \end{bmatrix}, \qquad \boldsymbol{y} = \boldsymbol{w}.\boldsymbol{X}$$

where:

- Vector $\boldsymbol{w}$ is accelerator sensor raw data collected at 6 stationary positions.
- Vector $\boldsymbol{y}$ is the known normalized Earth gravity vector.
- Matrix $\boldsymbol{X}$ is the 12 calibration parameters that is determined as below:

$$\boldsymbol{X} = \left[\boldsymbol{w}^T.\boldsymbol{w}\right]^{-1}.\boldsymbol{w}^T.\boldsymbol{y}$$

Based on the fixed sensor position, the data processing and analysis are performed on z-axis of the accelerometer. The accelerometer data is filtered through a 10th order Butterworth low pass filter with cutoff frequency 1 Hz. In the next part we are going to analyze the fluctuation of different breathing patterns resulted from five types of respiration disorders.

3 Detrended Fluctuation Analysis (DFA)

Detrended Fluctuation Analysis (DFA) quantifies fractal like auto-correlation properties of the signals [14]. It is generally accepted that the significant complexity of biological signals is due to two main factors [15] i.e. high complexity of systems and their susceptibility to environmental factors [14]. Biological signals are difficult to analyze because they are mostly non-stationary and from a wide range of physiological phenomena possess a scale invariant structure [16, 17]. Indeed, they have a scale invariant structure when the structure repeats itself on subintervals of the signal [17].

The validation of accelerometer driven respiration signal is investigated in [18] and the mean correlation of 0.84 which shows a very close correspondence of the accelerometer sensor and spirometer data is obtained. Therefore, here we make use of this result and DFA effectiveness is analyzed to discriminate healthy from pathological accelerometer driven respiration patterns.

DFA was first introduced by Peng et al. [19]; and Acharya et al. [20] uses DFA for disease classification in ECG studies. In many cases the DFA scaling exponent can be used to distinguish healthy and unhealthy data [21]. Indeed, DFA is a scaling analysis method that provides a simple quantitative parameter to represent the autocorrelation properties of a signal [19]. Thus, it could be a good feature to be utilized in the classification techniques. Figure 1, briefly summarized the proposed procedures.

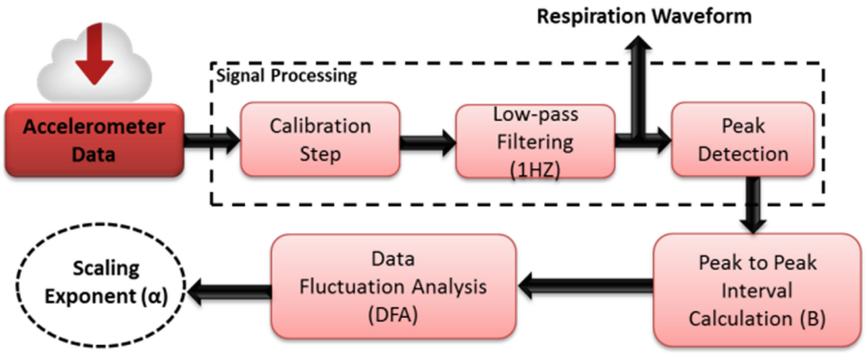

Fig. 1. Signal processing flowchart

3.1 DFA Algorithm

In the application of DFA to our extracted respiration signal, parameter B is the peak to peak *(P_P)* interval of breathing signal. We applied a peak detector algorithm which defined a customized threshold to decide whether each peak is significantly larger than the local data and then the peak intervals are calculated. B is first integrated in Eq. (1) to calculate the sum of the differences between the i_{th} P_P interval $B(i)$ and the mean P_P interval B_{ave}.

$$y(k) = \sum_{i=1}^{k} |B(i) - B_{ave}| \tag{1}$$

Next, as is shown in Fig. 2 for respiration signal, the integrated series $y(k)$ is divided into boxes of equal length n. Each box is subsequently detrended by subtracting a least square linear fit, denoted as $y_n(k)$.Then the Root Mean Square (RMS) of this integrated and detrended time series is obtained by:

$$F(n) = \sqrt{\frac{\sum_{k=1}^{N} [y(k) - y_n(k)]^2}{N}}$$

In the example in Fig. 2, n is equal to 3. The linear dependence indicates the presence of self-fluctuations and the slope of the line determines the scaling exponent α [17, 22]:

$$F(n) \sim n^{\alpha}$$

The parameter α (scaling exponent, autocorrelation exponent, self-similarity parameter) shows the autocorrelation properties of the signal [20, 23]:

1. $\alpha < 0.5$ anti-correlated signal
2. $\alpha = 0.5$ uncorrelated signal (white noise)
3. $\alpha > 0.5$ positive autocorrelation in the signal

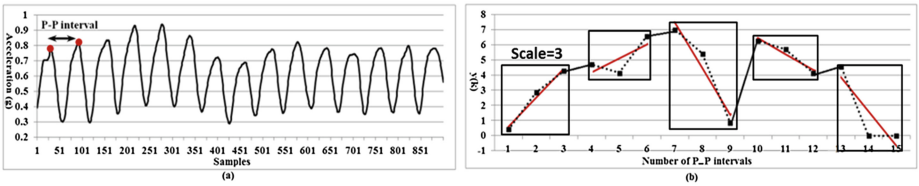

Fig. 2. (a) Original signal, (b) Integrated signal with trends

4. α = 1 Pink noise or 1/f noise
5. α = 1.5 Brownian noise or random walk.

Gifani et al. [14] claims that using scaling exponent α, one can completely describe the significant autocorrelation properties of the bio-medical signals. In this study, we use scaling exponent α of normal breathing as well as five different diseases.

4 Experimental Results

In our experiments, the acceleration signal was acquired with MEMS, KXTJ9, 3-axis low-power accelerometer with 12-bit resolution and sampling rate 50 HZ (Fig. 3(a)). The data is transmitted via CC2541 BLE, a new standard that allows Bluetooth equipment to run for long time on a single coin cell battery. It is worth noting that our node is fully radio type approved for US, Europe, Japan and Canada. The received sensors data are stored in the cloud in order to real-time or further analysis.

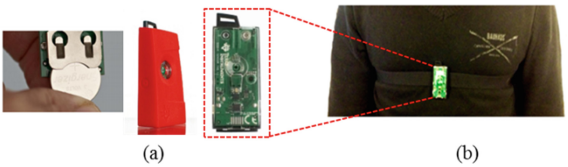

Fig. 3. (a) Sensory node, (b) Hardware module being worn

4.1 Test Setup

The participants of this study were five males and six females aged 4 to 48 with Mean ± SD, 26.54 ± 11.9026. They were instructed how to perform each breath exercise before their recording sessions. The experimental trials lasted for about 50 min per subject. We asked the subjects to perform Normal (N1), Bradapnea, Tachypnea, and Cheyn-stokes patterns, each for 2 min (6000 samples) and the other two types for 1 min with a 3 min rest interval. For simulating apnea in Cheyn-stokes and Biot's breathing exercises, we requested the participants to pause breathing for at least 3 s. Besides, for DFA analysis we asked our subjects to repeat normal breathing for another 1 min (N2). The sensor was mounted on the subject's chest in the middle of sternum region (Fig. 3(b)) and secured by a soft and elastic strap which is easy to attach and

comfortable to wear. In the trial session, the subjects were in the lying position; however, the rest positions or activities in which rib cage is stationary could be considered.

4.2 Breathing Patterns

In our test, the subjects are asked to perform six breathing patterns i.e., Normal, Bradapnea, Tachypnea, Cheyn-stokes, Kaussmal, and Biot's. Bradapnea is regular in rhythm but slower than normal in rate. Tachypnea is the condition of rapid breathing, with respiration rate higher than 20 respirations per minute (rpm). Tachypnea may occur due to physiological or pathological problems [24]. Cheyn-stokes breathing pattern is determined by gradually increasing, then decreasing the lung volume with a period of apnea. People suffering from central sleep apnea syndrome (CSAS) have the same breathing pattern at sleep [25]. Kussmaul which is defined as a rapid, deep and labored breathing type usually occurs in diabetics in diabetic ketoacidosis [26]. Biot's breathing is characterized by periods of rapid respirations followed by regular periods of apnea. There are different reasons which causes Biot's breathing, such as damage to the medulla oblongata by stroke (CVA) or trauma, or pressure on the medulla due to uncal or tentorial herniation and prolonged opioid abuse [26]. Figure 4 shows samples of all normalized patterns extracted from accelerometer sensor.

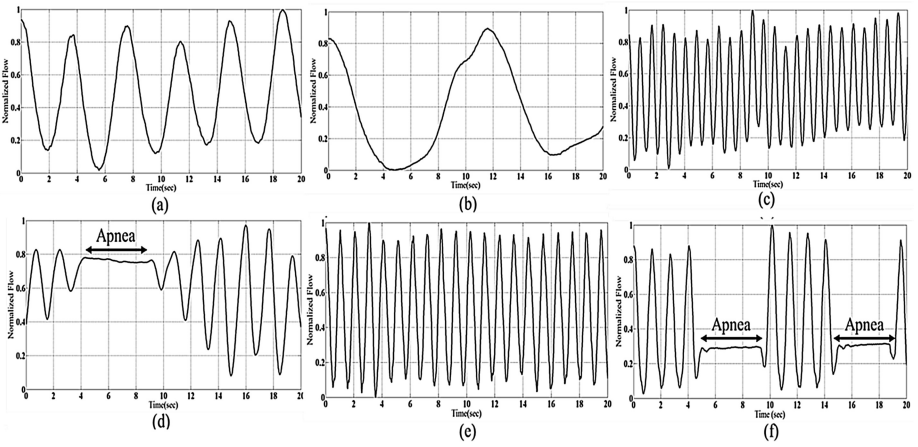

Fig. 4. (a) Normal (b) Bradapnea, (c) Tachypnea, (d) Cheyn-stokes, (e) Kussmaul and (f) Biot's breathing patterns extracted from accelerometer sensor.

4.3 DFA Analysis

In this section the respiration data are successfully analyzed using the DFA algorithm. Short-term data of 1-min duration for periods of normal and abnormal breathings and five scales 3, 4, 5, 6, and 7 are considered. The average fluctuations versus box-size are plotted in Fig. 5.

The graphs in Fig. 5 are for one of our subjects. It was observed that, each subject has its own signal characteristics based on the fluctuation analysis. It is worth noting that for all subjects, there is a difference in the average scaling exponent α of normal and abnormal respirations which helps us to use DFA as one of the effective features for healthy and unhealthy classification. This difference is various for different types of disorders and in some cases we can see the higher diverse which results in more reliable distinction. As a sample in Fig. 5, the blue and red lines are two normal patterns which obviously resulted in parallel lines (equal slope) while the black lines depict the specific disorders with different slopes. Table 1 shows the obtained scaling exponent for the whole population and patterns. Considering object 1, her normal respiration signal based on α is an anti-correlated signal shown in Fig. 5(a).

According to the obtained results in Fig. 5, the Kaussmal and Biot's respiration signals are close to white noise while for Bradapnea and Cheyn-stokes breathing models, the signals are included in positive autocorrelation category. Her Tachypnea breathing is close to Pink noise in which the power spectral density is inversely proportional to the frequency of the signal. The absolute differences of scaling exponents of N2 and abnormal patterns with respect to N1 are presented in Fig. 6(a).

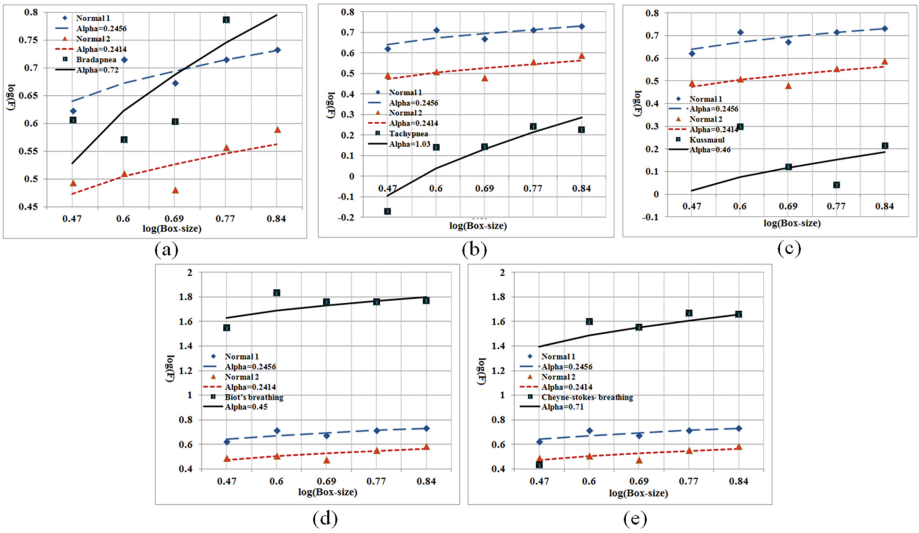

Fig. 5. Scaling exponents for (a) two Normal breathing and Bradapnea, (b) Tachypnea, (c) Kaussmaul, (d) Biot's and (e) Cheyn-stokes breathing patterns

It can be also seen in Fig. 6(b) that for all subjects, the greater mean differences are belong to the abnormal patterns while the differences of the second normal breathing are very close to zero. If we consider all subjects and breath patterns, α differences of abnormal breathings and N2 with regard to N1 are 0.51 ± 0.19 and 0.05 ± 0.04, respectively. Therefore, we conclude that DFA on respiration signals is a good and simple criterion to be used as an important feature in breath disorders detection.

Table 1. Scaling exponent (Alpha) for all subjects and different patterns

Subjects ID	Gender/ Age	Normal 1(N1)	Normal 2(N2)	Bradapnea	Tachypnea	Kussmaul	Biot's	Cheyn-stokes
1	**M/48**	0.24	0.24	0.72	1.03	0.46	0.45	0.71
2	**F/37**	0.96	1.05	0.44	0.17	1.19	0.82	1.71
3	**M/30**	0.39	0.32	0.61	0.82	1.02	0.86	0.83
4	**M/29**	1.30	1.29	2.61	0.14	1.19	0.10	0.94
5	**F/28**	0.22	0.15	0.36	0.70	0.64	0.35	0.07
6	**F/28**	0.60	0.60	0.34	0.83	0.84	0.39	0.70
7	**F/28**	1.22	1.15	1.50	0.82	1.42	1.40	2.74
8	**F/27**	1.37	1.46	0.53	0.76	1.09	2.38	0.66
9	**F/24**	0.82	0.75	0.30	0.45	1.010	1.00	2.15

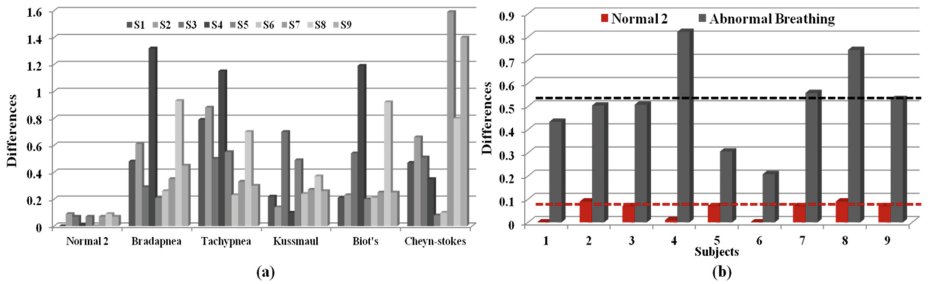

Fig. 6 (a) The absolute differences of scaling exponents of N2 and abnormal patterns with respect to N1 (b) The mean differences of scaling exponents (all 5 types of breath disorders)

5 Conclusion

In this paper, we presented a respiration monitoring system as well as applying the detrended fluctuation analysis on the accelerometer driven respiration signal. The results revealed the potential of remote diagnosis based on accelerometer sensor as a simple, convenience and low-cost method. In this platform, the physicians are able to share information together and precisely diagnosis the breathing diseases as well as monitoring the patient's progressing in performing the prescribed breathing exercises in respiratory therapy wherever they are with devices such as an iPhone, iPad or the web regardless of their proximity to the patients.

Therefore, early identification through this portable monitoring system and timely treatment of exacerbations can decrease the hospital admissions and slow deterioration while reducing early mortality and disease costs [27].

References

1. Bannister, R., Cunningham, D.: The effects on the respiration and performance during exercise of adding oxygen to the inspired air. J. Physiol. **125**, 118–137 (1954)

2. Zhu, X., Chen, W., Nemoto, T., Kanemitsu, Y., Kitamura, K., Yamakoshi, K., Wei, D.: Real-time monitoring of respiration rhythm and pulse rate during sleep. IEEE Trans. Biomed. Eng. **53**, 2553–2563 (2006)
3. Mann, J., Rabinovich, R., Bates, A., Giavedoni, S., MacNee, W., Arvind, D.K.: Simultaneous activity and respiratory monitoring using an accelerometer. In: International Conference on Body Sensor Networks (BSN), pp. 139–143, May 2011
4. Neuman, M.R., Watson, H., Mendenhall, R.S., Zoldak, J.T., Di Fiore, J.M., Peucker, M., Baird, T.M., Crowell, D.H., Hoppenbrouwers, T.T., Hufford, D., Hunt, C.E., Corwin, M.J., Tinsley, L.R., Weese-Mayer, D.E., Sackner, M.A.: Cardiopulmonary monitoring at home: the CHIME monitor. Physiol. Meas. **22**(2), 267–286 (2001)
5. Lindberg, L.G., Ugnell, H., Oberg, P.A.: Monitoring of respiratory and heart rates using a fibre-optic sensor. Med. Biol. Eng. Comput. **30**(5), 533–537 (1992)
6. Matthews, G., Sudduth, B., Burrow, M.: A noncontact vital signs monitor. Crit. Rev. Biomed. Eng. **28**(1–2), 173–178 (2000)
7. Moody, G.B., Mark, R.G., Zoccola, A., Mantero, S.: Derivation of respiratory signals from multi-lead ECGs. Proc. Comput. Cardiol. **12**, 113–116 (1985)
8. de Chazal, P., Heneghan, C., Sheridan, E., Reilly, R., Nolan, P., O'Malley, M.: Automated processing of the single-lead electrocardiogram for the detection of obstructive sleep apnoea. IEEE Trans. Biomed. Eng. **50**(6), 686–696 (2003)
9. Dobrev, D., Daskalov, I.: Two-electrode telemetric instrument for infant heart rate and apnea monitoring. Med. Eng. Phys. **20**(10), 729–734 (1998)
10. Bates, A., Ling, M., Geng, C., Turk, A., Arvind, D.K.: Accelerometer-based respiratory measurement during speech. In: International Conference on Body Sensor Networks (BSN), pp. 95–100, May 2011
11. Dehkordi, P.K., Marzencki, M., Tavakolian, K., Kaminska, M., Kaminska, B.: Validation of respiratory signal derived from suprasternal notch acceleration for sleep apnea detection. In: International Conference of the IEEE on Engineering in Medicine and Biology Society EMBC, pp. 3824–3827 (2011)
12. Tilt measurement using a low-g 3-axis accelerometer, Application note, STMicroelectronics group of companies (2010)
13. Fekr, A.R., Janidarmian, M., Sarbishei, O., Nahill, B., Radecka, K., Zilic, Z.: MSE minimization and fault-tolerant data fusion for multi-sensor systems. In: IEEE 30th International Conference on Computer Design (ICCD), pp. 445–452 (2012)
14. Gifani, P., Rabiee, H.R., Hashemi, M.H.: Optimal fractal-scaling analysis of human EEG dynamic for depth of anesthesia quantification. J. Franklin Inst. **344**, 212–229 (2007)
15. Kushida, C.A., Littner, M.R., Morgenthaler, T., Alessi, C.A., Bailey, D., Coleman, J., Friedman, L., Hirshkowitz, M., Kapen, S., Kramer, M., Lee-Chiong, T., Loube, D.L., Owens, J., Pancer, J.P., Wise, M.: Practice parameters for the indications for polysomnography and related procedures: an update for 2005. Sleep **28**(4), 499–521 (2005)
16. Gifani, P., Rabiee, H.R., Hashemi, M.H.: Optimal fractal-scaling analysis of human EEG dynamic for depth of anesthesia quantification. J. Franklin Inst. **344**, 212–229 (2007)
17. Lee, J.M., Kim, D.J., Kim, I.Y.: Detrended fluctuation analysis of EEG in sleep apnea using MIT/BIH polysomnography data. Comput. Biol. Med. **32**, 37–47 (2002)
18. Fekr, A.R., Janidarmian, M., Radecka, K., Zilic, Z.: A medical cloud-based platform for respiration rate measurement and hierarchical classification of breath disorders. Sensors **14** (6), 11204–11224 (2014)
19. Peng, C.K., Havlin, S., Stanley, H.E., Goldberger, A.L.: Quantification of scaling exponents and crossover phenomena in nonstationary heartbeat time series. Chaos **5**, 82–87 (1995)
20. Acharya, R.U., Lim, C.M., Joseph, P.: Heart rate variability analysis using correlation dimension and detrended fluctuation analysis. ITBM-RBM **23**(6), 333–339 (2002)

21. Rodriguez, E., Echeverria, J.C., Alvarez-Ramirez, J.: Detrended fluctuation analysis of heart intrabeat dynamics. Phys. A **384**, 429–438 (2007)
22. Ihlen, E.A.F.: Introduction to multifractal detrended fluctuation analysis in matlab. Front Physiol. **3**(141) 4 June 2012
23. Wilkinson, T.M.A., Donaldson, G.C., Hurst, J.R., Seemungal, T.A.R., Wedzicha, J.A.: Early therapy improves outcomes of exacerbations of chronic obstructive pulmonary disease. Am. J. Respir. Crit. Care Med. **169**(12), 1298–1303 (2004)
24. William, H., Myron, L., Robin, D., Mark, A.: Current Diagnosis and Treatment in Pediatrics. 21 edn., McGraw-Hill Professional, New York City, p. 989
25. Kumar, P., Clark, M.: "13". In: Clinical Medicine, 6 edn., p. 733. Elsevier Saunders, Philadelphia (2005). ISBN 0-7020-2763-4
26. Farney, R.J., Walker, J.M., Boyle, K.M., Cloward, T.V., Shilling, K.C.: Adaptive servoventilation (ASV) in patients with sleep disordered breathing associated with chronic opioid medications for non-malignant pain. J. Clin. Sleep Med. **4**(4), 311–319 (2008). PMC 2542501. PMID 18763421
27. Wilkinson, T.M.A., Donaldson, G.C., Hurst, J.R., Seemungal, T.A.R., Wedzicha, J.A.: Early therapy improves outcomes of exacerbations of chronic obstructive pulmonary disease. Am. J. Respir. Crit. Care Med. **169**(12), 1298–1303 (2004)